

## UV-ABSORPTION MECHANISMS OF Ni<sup>2+</sup>-BINDING BOVINE SERUM ALBUMIN

M. DIEACONU, A. IOANID\*, S. IFTIMIE, S. ANTOHE

*University of Bucharest, Faculty of Physics, 405 Atomistilor Street, PO Box MG-11, 077125, Magurele-Ilfov, Romania*

Interactions proteins-metalic ions are a major concern in various emerging fields like bionanotechnology and material sciences. Nickel is known to be an essential element for the living organisms those deficiencies cause allergic reactions, dermatitis, asthma, and also can induce carcinogenesis. Although it is known that binds to albumin, his physiological role is not complete established. Certainly, this role must be connected to the intimate physical and electrochemical features of the binding process. We present any new results concerning the binding process of Ni<sup>2+</sup> on BSA, according to the UV absorbance spectrum structure of the [BSA:Ni<sup>2+</sup>][1:1]M system, with concentration  $(0.01 \div 1) \times 10^{-4} M$ , in buffer phosphate solution having pH-value neighbouring the physiological values.

(Received June 10, 2012; Accepted August 1, 2012)

*Keywords:* bovine serum albumin, transition metal complex symmetry, molecular orbital, electronic transitions, charge transfer transitions

### 1. Introduction

Living organisms grow, differentiate, reproduce, and respond to their environment via specific and integrated interactions between biomolecules, as those between an enzyme and its substrate or inhibitor, a hormon or growth factor and its receptor, an antibody and its antigen, or, indeed, the binding of effector molecules or of ions. For proteins case, the last two interactions act as denaturants because induce the changes of the secondary (short-range folding) and tertiary (long-range folding) structure, so that occur the important functionality changes. The common parameters that assist an understanding and a measure of the biochemical effect of the any interactions are the binding affinity, binding specificity, number of binding sites per molecule, as well as the enthalpic and entropic contributions to the binding energy.

Serum albumin (bovine serum albumin-BSA and hers human omologue, human serum albumin-HSA) is the one of the most important blood proteins, with a concentration of about 0.63 mM, and is a versatil carrier protein, active against a variety of exogen agents with widely differing properties, as small hydrophobic or hydrophilic molecule, positive or negative ions, normal or transition metal ions, anionic or cationic radicals, as well as drugs and xenobiotics [1].

The reactivity of the tranzition metals depends equally on the ligands, coordination geometry and oxidation state of the metal. Biological systems have taken advantage of the transition metals' reactivity by coordinating the metals in the framework of a protein structure that controls the reactivity and oxidation states of the metal.

Serum albumin possesses the capacity of reversible binding of a great number of substances, including bilirubin, hormones, drugs and ions. Transition metal ions catalyze a variety of biological reactions essential to sustain life. The albumin-ion interactions might influence the absorbtion, transport, metabolism and excretion of ions [2].

---

\* Corresponding author: ana\_ioanid@yahoo.com

Physicochemical studies directed to the determination of the tertiary structure and solution conformation have been based on the interpretation of the protein solution hydrodynamics at neutral pH [3], the phosphorescence depolarization, circular dichroism (CD) and electronic absorption spectroscopy (UV-VIS), FTIR, atomic force microscopy (AFM) [4,5] for both free and binding albumin.

The conformation of a protein in water solution, as shape and sizes, is generally a function of electrostatic, hydrogen-bonding, van der Waals, and hydrophobic interactions among the amino acid residues that all specifically favor unique conformation of protein in solution, termed the native state, whereby the charged and polar (hydrophilic) amino acid groups are exterior and exposed to water, while the nonpolar moieties (hydrophobic) generally reside in interior of folded structure, protected from destabilizing solvent interactions.

The BSA macromolecule has a large number of charged amino acids on the surface, so that has a net charge of (-18) at neutral conditions [1].

The metallic ions bind strongly to protein through electrostatic interactions with surface charged amino acids. The net charge of protein is changed and as a result, the protein structure adapts to a new equilibrium conformation, with other amino acids exposed to solvent.

Knowledge of the behaviour of the protein in a given solvent, particularly in water solution is the main goal of the research in the design and delivery drugs.

Interactions proteins-metallic ions are a major concern in various emerging fields like bionanotechnology and material sciences. Thus, the bare malachite ( $\text{Cu}_2(\text{OH})_2\text{CO}_3$ ) nanoparticle and BSA-malachite nanocomposite have been used for the adsorption of a series of toxic and precious metal ions from single- and multicomponent aqueous solution. The nanocomposites obtained by the surface modification of the malachite nanoparticles with BSA, have the differentiated absorption behavior for the same series of metal ions [6].

Nickel is known to be an essential element for the living organisms, but any deficiencies induced in animals by dietary deprivation of  $\text{Ni}^{2+}$ , cause allergic reactions, dermatitis, asthma, and also can induce carcinogenesis [7].

In vivo, a substantial proportion of injected  $\text{Ni}^{2+}$  by nourishment or medicine way, binds to albumin, but his physiological rôle is not completely established.

We present any new results concerning the binding process of  $\text{Ni}^{2+}$  on BSA, according to the UV absorbance spectrum structure of the  $[\text{BSA}:\text{Ni}^{2+}][1:1]\text{M}$  system, with concentration  $(0.01 \div 1) \times 10^{-4}\text{M}$ , in buffer phosphate solution having pH-value neighbouring the physiological values.

## 2. Free and binding BSA structure

Bovine serum albumin (BSA) is a single-chain protein that, in the folding (native) state, has a tertiary structure characterized by a unique arrangement of three globular domains, I,II,III, each comprising two smaller subdomains A and B, stabilized by an internal network of disulfide bonds and each bearing a number of ionizable groups with opposite signs. Hydrodynamic measurements of sedimentation coefficients and rotational relaxation time, low-angle X-ray scattering and neutron scattering [8] indicate that the BSA molecule in solution has a prolate ellipsoidal shape with a molecular weight of 66.700kDa. BSA molecule is built from 583 amino acid residues. For physiological value of pH (~7.4), the BSA secondary structure consists to 67%  $\alpha$ -helix, 10% turn, and 23% extended chain (but not  $\beta$ -sheet) [9,10]. In solution, the multiple binding sites on exposed surface of molecule, assures the exceptional ability of BSA to interact with many organic and inorganic molecules, drugs, ionic metals and radicals. All these interactions induce configurational transitions and secondary structure changes, that, in reasonable proportions, are reversible and give flexibility and versatility to function of protein.

Protein unfolding can be induced by a variety of external conditions: pH-solution changes produce the ionization of nonpolar residues, temperature variations control the complex interplay between caloric and structural effects, and chemical denaturant, as surfactants, ions, small molecules interact preferentially with the polar (bind strongly to protein by electrostatic interactions with oppositely charged amino acids) or non-polar (hydrophobic interactions) amino acids. As a

result, denaturant binding enhanced protein unfolding by aggregation or coalescence via surface coverage of new chemical complexes [11] or via exposure of the core protein hydrophobic amino acids.

Albumins have a high affinity metal binding sites, but the effectiveness in binding metal ions depends on the protein configuration because each metal ion has a preferential coordination with the coordinating side-chain of amino acids in proteins. Such, because any secondary structural elements are reduced compared to native state, BSA exhibits a reverse preferential binding capacity for  $\text{Au}^{3+}$ ,  $\text{Pd}^{2+}$ ,  $\text{Hg}^{2+}$ ,  $\text{Ag}^+$  (soft metal ions) compared to  $\text{Cr}^{3+}$ ,  $\text{Ni}^{2+}$ ,  $\text{Zn}^{2+}$ ,  $\text{Cu}^{2+}$  (hard metal ions) then is denaturated by adsorption on malachite nanoparticles [6].

Electronic spectrum of the  $\text{Ni}^{2+}$ -complexes in solution shows that, as in solid crystal,  $\text{Ni}^{2+}$  ion having the electronic structure  $[\text{Ar}] (3d^8 4s^0)$ , forms the square-coplanar diamagnetic complexes with donor ligands as nitrogen or oxygen [12].

The NMR results [7] demonstrate that  $\text{Ni}^{2+}$  binds at the N-terminal sites of both HSA and BSA in solution. Any significant chemical shift differences between bound and free albumin resonances have been observed, indicating a strong binding that depends of  $\text{Ni}^{2+}$ -concentration. On addition  $\text{Ni}^{2+}$  in solution, the end point for disappearance of BSA resonances and the appearance of BSA-Ni resonances is close to [1:1] M ratio, while for HSA-Ni is close to [1:0.8] M ratio. Thus, using  $^1\text{H}$ -NMR spectroscopy is possible to probe the binding of  $\text{Ni}^{2+}$  to the N-terminal of the Asp1, His3, Lys4 hydrophilic residues and Ala2 (or Thr2) amphiphilic residue, namely  $\alpha\text{N}$ -terminal of Asp1 and Ala1(or Thr2),  $\varepsilon\text{N}$ -terminal from  $\text{NH}_2$  side-chain of Lys4 and  $\delta\text{N}$ -terminal from imidazole side-chain of His3.

The stoichiometry for  $\text{Ni}^{2+}$  as ligand binding to BSA as receptor, is close to [1:1]M ratio, consistent with a single binding site.

Experimental results about behaviours of interactions between  $\text{Ni}^{2+}$  ion and human and bovine serum albumin for a [1:1]M system, show that the binding of the first  $\text{Ni}^{2+}$  on protein induce a slow conformational changes that afterwards favorize cooperative binding processes [13].

### 3. Experimental results

#### 3. 1. UV-spectra

We present an analysis of the UV-absorbance spectra of the  $1 \times 10^{-4} \text{M}$   $[\text{BSA}:\text{Ni}^{2+}][1:1]\text{M}$  in phosphate buffer solution for  $(200 \div 350)\text{nm}$  range of

wavelength. BSA with electrophoretic purity were purchased from Sigma Laboratories and for  $\text{Ni}^{2+}$  ligands were used nickel chlorate p.a. ( $\text{NiCl}_2$ ) from Reactivul Laboratories, Romania.

All samples were prepared with the phosphate buffer solutions containing 8 g NaCl, 0.2g KCl, 1.44 g  $\text{Na}_2\text{HPO}_4$ , 0.24g  $\text{KH}_2\text{PO}_4$  and distilled water for  $1000\text{cm}^3$  solution. The pH-value has been adjusted to  $(7 \div 7.4)$  with NaOH 0.1M solution. BSA (66.430 mg) and  $\text{NiCl}_2$  (0.130 mg) was been dissolved in  $10\text{cm}^3$  of phosphate buffer solution for  $1 \times 10^{-4} \text{M}$   $[\text{BSA}:\text{Ni}^{2+}][1:1]\text{M}$  sample.

The difference absorbance spectra between  $1 \times 10^{-4} \text{M}$   $[\text{BSA}:\text{Ni}^{2+}][1:1]\text{M}$  sample cell and  $1 \times 10^{-4} \text{M}$  [BSA] reference cell, were recorded using a Perkin Almer Lambda 35 Spectrofotometer in  $(190 \div 1100)\text{nm}$  spectral range. All samples were characterized at room temperature under ambient conditions.

The changes of spectrum of the  $[\text{BSA}:\text{Ni}^{2+}][1:1]\text{M}$  system compared to the free BSA, depend on  $[\text{Ni}^{2+}]$  in solution, but any significant changes appear for  $[\text{Ni}^{2+}] \sim 1 \times 10^{-4} \text{M}$ . The Fig.1 shows the absorbance spectra of the  $1 \times 10^{-6} \text{M}$  [BSA] (1),  $1 \times 10^{-4} \text{M}$  [BSA] (2) and  $1 \times 10^{-4} \text{M}$   $[\text{BSA}:\text{Ni}^{2+}][1:1]\text{M}$  (3).

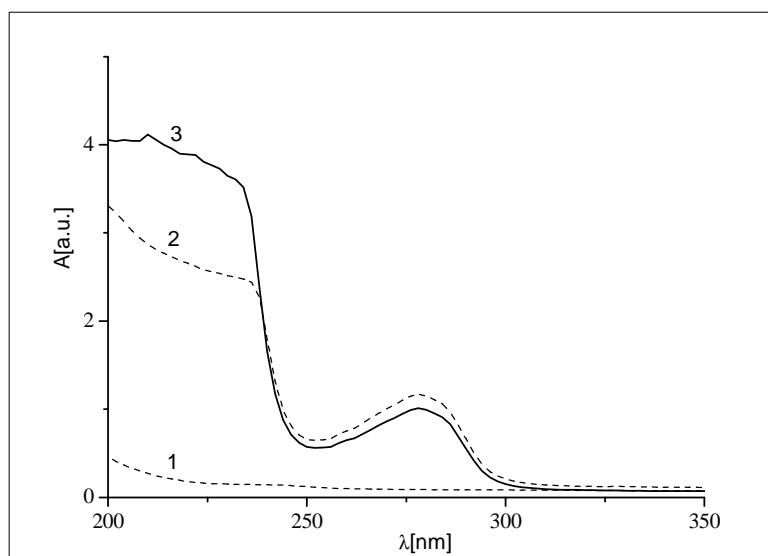


Fig.1. Normal absorbance spectra: (1)  $1 \times 10^{-6} M$  [BSA]/air; (2)  $1 \times 10^{-4} M$  [BSA]/air; (3)  $1 \times 10^{-4} M$  [BSA:  $Ni^{2+}$ ] [1:1]/air

For the identification of the relevant absorbance peaks, in Fig.2 we show the second derivative spectra both of  $1 \times 10^{-4} M$  [BSA] and  $1 \times 10^{-4} M$  [BSA:  $Ni^{2+}$ ] [1:1]M systems. The second derivative spectroscopy is useful since peaks and shoulders of the original absorbance spectra are transformed into negative peaks having the minima centered at the same wavelength. Thus any minor spectral features are detected with an extremely low or negligible error [14].

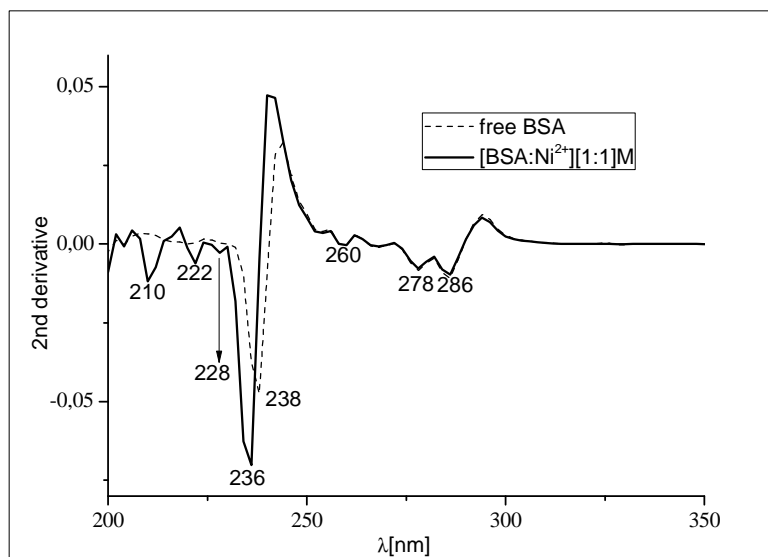


Fig.2. Second derivatives of spectra shown in Fig.1: (dash)  $1 \times 10^{-4} M$  [BSA]/air; (solid)  $1 \times 10^{-4} M$  [BSA:  $Ni^{2+}$ ] [1:1]M /air.

### 3.2. UV-absorption mechanisms of protein

It is known that the proteins absorb UV light with two distinct peaks. The peak centered on  $\lambda = 278 \text{ nm}$  is result of absorbance by aromatic ring portion of their structure (tryptophan, tyrosine, phenylalanine hydrophobic amino acids), while the peak at lower wavelength  $\lambda \sim 230 \text{ nm}$  is caused by absorbance of peptide and carboxylic acid moieties in the compounds (N-terminal peptide as  $-\text{NH}-\text{CHR}-\text{COOH}$  and C-terminal peptide as  $\text{NH}_2-\text{CHR}-\text{CO}-$ ). In peptides, the chromophore which interacts with light is the amide group (Fig.3(a)) that possess a conjugated system spread over the O,C and N atoms, consisting of molecular orbitals occupied by delocalized electrons. Thus, amide group absorbs by his  $\pi^0 \rightarrow \pi^*$  and  $\pi \rightarrow \pi^*$  electronic transitions.

UV-absorbance spectrum of free BSA in phosphate buffer solution having concentration and pH- value neighbouring the physiological values, shows two bands, one weak as a should centered on  $\lambda = 278 \text{ nm}$  and one intense and large, between  $\lambda \sim 240 \text{ nm}$  and  $\lambda \sim 200 \text{ nm}$ . The same spectrum but for the BSA aggregated by addition of a salt and exposing their hydrophobic patches to water, shows hypochromism [15].

Since a typical polypeptide has hundreds of amide groups one could expect optical transitions to have very broad absorption bands. As for a crystal, it is possible to chose a structural unit, with a smaller number of chromophores that will generate the whole array by simple translation.

The unit cell of a isolated  $\alpha$ -helix contains maximum two amide bonds, while the these of a  $\beta$ -pleated sheet conformation, parallel or antiparallel, contains four amide bonds. So that, the theoretical electronic transition for  $\alpha$ -helix can be split in maximum two transitions and for  $\beta$ -sheet in maximum four transitions. In order for a electronic transition to occur it is necessary that a charge moves, or that a dipole be created. The electronic transition is forbidden if a dipole cannot be created. Thus, the optical transitions observed are those that are in phase with each other, and the induced total dipole moment of the unit cell is non-zero.

The induced dipole moment is defined by  $\hat{d} = e(\sum_i x_i, \sum_i y_i, \sum_i z_i)$  and the transition dipole moment  $\hat{D}$  is defined by

$$D_{nm} = \int \psi_n^* \hat{d} \psi_m d\vec{r} = \langle \psi_n | \hat{d} | \psi_m \rangle$$

and represents the oscillator strenght for the optical absorption between initial state  $m$  and final state  $n$  of molecule. The direction of  $\hat{D}$  in the molecular space defines the direction of transition polarization. Because  $\hat{d}$  is an odd function, the tranzition dipole moment  $D_{nm}$  is the even function (allowed) if the initial state  $m$  and final  $n$  differ by their parity, e.g., one is even ( $g$ -symmetry) and other is odd ( $u$ -symmetry).

In the geometry of  $\alpha$ -helix conformation, the transition moment vectors of the unit cell lie approximately along the sides of a square inclined from the helix by the dihedral specific constraints. The total transition moment has two components, parallel and perpendicular to helix.

In the  $\beta$ -pleated sheet conformation, the transition moment vectors are placed into an array and the total transition moment has two components, parallel and perpendicular to sheet.

The stabilization of the final molecule structure is assured by the dipole -dipole interaction between pair of chromophores that has known form:

$$V_{ij} = \frac{1}{4\pi\epsilon_0\epsilon} \frac{|\vec{d}_i||\vec{d}_j|}{R_{ij}^3} [\vec{e}_i \cdot \vec{e}_j - 3(\vec{u} \cdot \vec{e}_i)(\vec{u} \cdot \vec{e}_j)]$$

where  $\epsilon_0$  is the vacuum permittivity,  $\epsilon$  is the medium permittivity,  $\vec{d}_i$  is the transition dipole moment of site  $i$ ,  $\vec{u}$  is the unit vector of the  $R_{ij}$  distance between the centers of dipoles in sites  $i$  and  $j$ , and  $\vec{e}_i$  is the unit vector of the transition moment of site  $i$ . In  $\alpha$ -helix the transition dipole

moment of Amide I group has the intensity of 0.3 D and makes an angle of  $17^\circ$  away from the CO bond and in the direction of the CN bond [16,17].

The dipole-dipole interaction depends on the relative orientation of the pair chromophore moments; when the chromophores are aligned side by side (as in  $\alpha$ -helix conformation), the dipole-dipole interaction reduces the energy of transition and as result the absorbance spectrum will show hypochromism for this transition. Then the chromophores are aligned tail to tail, the dipole-dipole interaction increases the transition energy and the absorbance will show hyperchromism.

The transition intensity of the amide group in  $\alpha$ -helix conformation of the molecule is greater than then this group is into  $\beta$ -pleated sheet conformation and the absorbance peak position shifts to red in the same conditions.

Electronic transitions in [BSA: Ni<sup>2+</sup>] system induce the specific dipole moments those complex-dipole – complex-dipole interaction one part, complex-dipole –chromophore-dipole interaction on the other hand, will stabilize a new equilibrium conformation for protein.

### 3.3. UV-spectrum structure

Main features of the absorbance behaviour that take off from the above UV spectra show that the absorbance of the [BSA: Ni<sup>2+</sup>][1:1]M system is significantly modified from 1M [BSA] for all wavelength range. Thus, i) for  $\lambda > 250 \text{ nm}$ , the absorbance of the [BSA: Ni<sup>2+</sup>][1:1]M system decreases in relation to 1M [BSA], while for  $\lambda < 250 \text{ nm}$  the behavior reverses, Fig.1. For the same solvent, the binding Ni<sup>2+</sup> to protein induces hypochromic effect for  $\lambda > 250 \text{ nm}$  and produces an increase and the appearance of new absorptions for  $\lambda < 250 \text{ nm}$ ; ii) the absorbance peak of the free protein at  $\lambda = 238 \text{ nm}$ , slowly blue shifts to  $\lambda = 236 \text{ nm}$  for the absorbance of [BSA: Ni<sup>2+</sup>][1:1]M system; iii) the new three peaks appear in the [BSA: Ni<sup>2+</sup>][1:1]M spectrum, namely, one relative intense at  $\lambda = 210 \text{ nm}$ , and two weak at  $\lambda = 222 \text{ nm}$  and  $\lambda = 228 \text{ nm}$ , Fig.2, all placed in the spectral range of the  $\pi^0 \rightarrow \pi^*$  and  $\pi \rightarrow \pi^*$  transitions of the amide group.

The significative quantitative changes of the absorbance in the  $\lambda < 250 \text{ nm}$  range, indicate that the binding of the Ni<sup>2+</sup> to BSA induces important changes in the excited states of protein.

The high intensity of the peak centered on  $\lambda = 236 \text{ nm}$  indicates that one may be assigned to a transition that is electric dipole-allowed, but is not d-d transition [12].

Despite their comparative weakness, the last three peaks at  $\lambda < 236 \text{ nm}$ , can't be assigned to d-d transitions that lie at  $\lambda > 350 \text{ nm}$  for all square-planar, tetrahedral and octahedral Ni<sup>2+</sup>-complexes in solutions [23].

All these observations suggest that the main observed absorbance bands relate the spectral behaviour of any Ni<sup>2+</sup>-complexes and may be assigned to any charge-transfer transitions which involve both the Ni<sup>2+</sup> and the complexed ligands. Electronic excitations in molecules involving the charge transfer usually occasion changes in bond lengths and frequently in molecular symmetry. Then an electron is excited from a weakly anti-bonding (or non-bonding) orbital to a strongly antibonding orbital, results in a significant change in molecular dimensions, with consequences for their dynamics.

## 4. Model

To discuss the source and energy positions of the observed absorbance bands, we propose a model for binding the Ni<sup>2+</sup> complexes with BSA in solution starting from symmetry theory considerations and energy arguments from the molecular orbital formalism.

Starting from the above NMR results [7], we propose following model for a square-coplanar diamagnetic complex  $[\text{Ni}^{2+}\text{N}_4]$ , those four N-terminal ligands are two  $\alpha\text{N}$ , one  $\varepsilon\text{N}$  and one  $\delta\text{N}$ .

#### 4.1. Forming and structure of the $\text{Ni}^{2+}$ -complexes in $[\text{BSA}:\text{Ni}^{2+}]$

The affinity of nickel for nitrogen ligands permits the  $\text{NH}_2$  group of protein to bind, but any specific geometries of coordinations are favoured by solvent [18]. The formation of the  $[\text{Ni}^{2+}\text{N}_4]$  complex is due to the affinity of nickel for the nitrogen lone pair electron. The  $\text{Ni}^{2+}$  ion as an electron deficient form of nickel atom interacts with nitrogen lone pair as donor, via resonance interactions (bonding) or inductive interactions (splitting due to electrostatic field of ligands). The amount of participation of the lone pair of N does depend critically on the geometry at N atom [19].

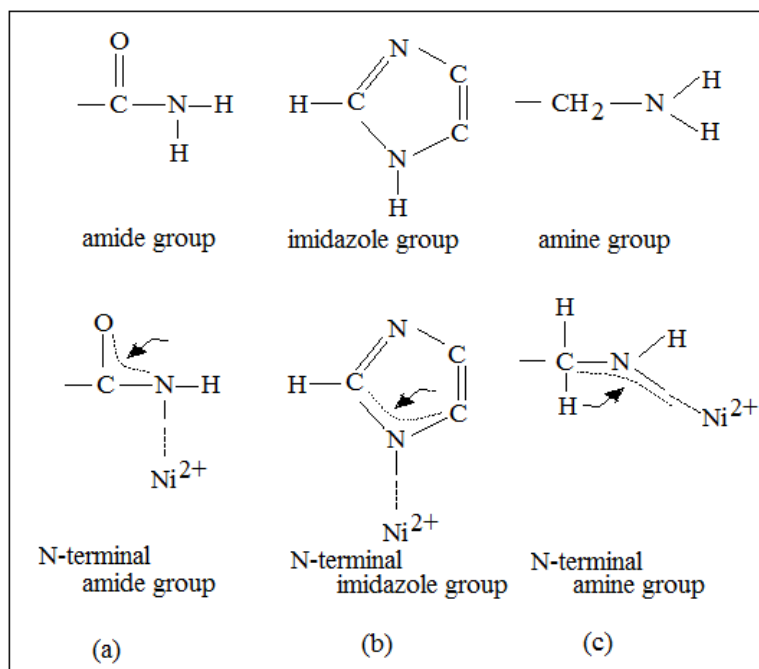


Fig.3. Ligand groups of  $[\text{Ni}^{2+}\text{N}_4]$ -square planar complex in  $[\text{BSA}:\text{Ni}^{2+}]$ : (a) N-terminal of amide bond; (b) N-terminal of imidazole group; (c) N-terminal of amine group. The arrow shows the sharing lone pair of nitrogen.

**Amide group**, (Fig.3(a)). In simplified molecular orbital theory, the  $2P_x$  orbitals of N ( $2s^2 2p^3$ ), C ( $2s^2 2p^2$ ) and O ( $2s^2 2p^4$ ) atoms of this group (containing 6 electrons and having the plane of the peptide bond as their nodal plane), are combined to form three orthogonal linear combinations corresponding to  $\pi$  bonding (filled with 2 electrons),  $\pi^0$  non-bonding (filled with 2 electrons) and  $\pi^*$  antibonding (empty) states. The remaining two electrons fill the non-bonding orbital  $2P_y$  of the oxygen atom [20].

The electronic transitions of the amide bond are affected by solvent and environment. Thus, the  $\pi^0 \rightarrow \pi^*$  transition blue shifts in water compared with organic solvent, while the  $\pi \rightarrow \pi^*$  transition red shifts in water because the excited state of this transition is more polar than the ground state. The  $\pi \rightarrow \pi^*$  transition of amide bond is a charge transfer from the N to O atoms (Fig.3a). The charged nitrogen forms a hydrogen bond with the aqueous solvent. Thus, the stabilization of the excited state leads to the effective lowering of the ionization potential of the amide. In unsaturated compound, as that above mentioned, in the frontier orbitals formalism, the

HOMO→LUMO excitation is generally a  $\pi \rightarrow \pi^*$  (or  $\pi^0 \rightarrow \pi^*$ ) transition, that for aqueous solution, occur in UV region, around  $\lambda \sim 240 \text{ nm}$ .

**Imidazole group**, (Fig.3(b)). The imidazole group is a cyclopentadiene anion those the HOMO's molecular orbitals are much higher in energy than those in neutral aromatic species such as benzen, so that is more capable of coordinating to transition metals with available empty d-orbitals. Absorption spectra of BSA in presence of the imidazole, show an increase of the absorbance and a blue shift the HOMO→LUMO excitation associated with  $\pi \rightarrow \pi^*$  transition, comparative to absence of the imidazole [21].

**Amine group**, (Fig.3(c)). The  $\pi \rightarrow \pi^*$  transition responsible for the amine-bond absorbance is placed around  $\lambda \sim 208 \text{ nm}$  (e.g., absorbance spectrum of poly-L-lysine) [22].

These remarks permit to suppose that both the imidazole group (Fig.3b) and the deprotonated N-terminal of lysine (Fig.3c), have greater energies for the  $\pi^*$  antibonding molecular orbital.

Although all the four ligands have same nature, the binding effects of  $\text{Ni}^{2+}$  on protein are intimating different, because the  $\alpha\text{N}$  ligands are directly bind to the back-bone chain of protein, while the  $\epsilon\text{N}$  ligand is the side-chain deprotonated  $\text{NH}_2$ -terminal of a lysine residue (Lys4) and  $\delta\text{N}$  ligand is the side-chain imidazole-terminal of a histidine residue (His3). Binding of  $\text{Ni}^{2+}$  to  $\alpha$ -nitrogen involves the change of their geometry in amide group and, consequently, change of the structural parameters of the protein molecule as their dipole moment, giration radius. As a result, the binding of  $\text{Ni}^{2+}$  induces the conformational changes of protein as the changes of relative proportions of  $\alpha$ -helix,  $\beta$ -sheet, and disordered forms of BSA in solutions containing  $\text{Ni}^{2+}$  ions [24,25].

Note that while the amide groups of the back-bone of protein are fixed by dihedral constrains, both side-chains imidazole and amine group have mobility each to other. Thus, while the inter-protonic distance  $d(\text{Asp}\alpha\text{-Ala}\alpha) \sim 0.44 \text{ nm}$  remains the same, the inter-protonic  $d(\text{Lys}\epsilon\text{-His}\delta)$  may be considerable larger than of  $d(\text{Lys}\epsilon\text{-His}\delta) \sim 0.32 \text{ nm}$  determined from a model based to crystal structure of system [25].

Taking into account these considerations, is more probable the trans-disposition than cis-disposition of the two  $\alpha\text{N}$  ligands (along to diagonal) that preserves the square planar configuration of the complex. This structure remains the same under the symmetry operations ( $E$ ,  $C_2(x,y,z)$ ,  $\sigma(xy, xz, yz)$ ,  $i$ ) of the  $D_{2h}$  point group.

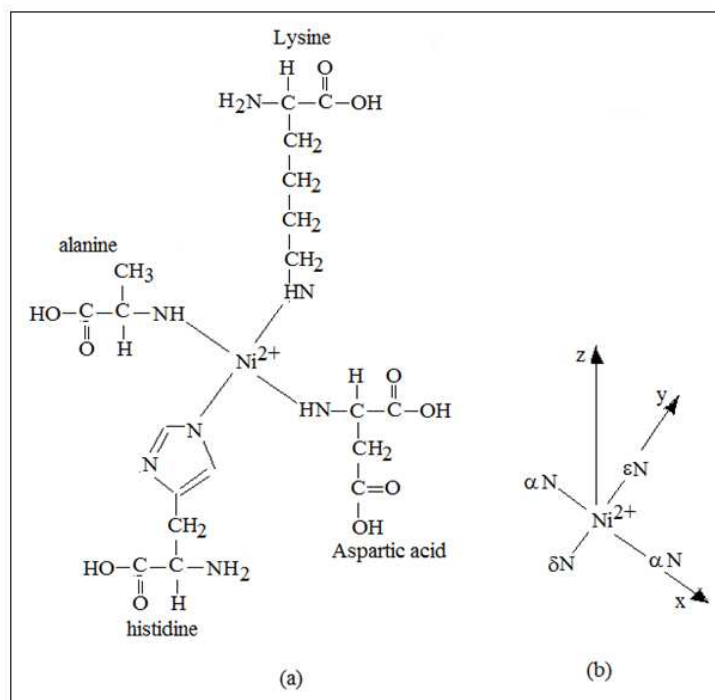


Fig. 4. Schematic structure of the square-coplanar  $[Ni^{2+}N_4]$  complex in  $[BSA: Ni^{2+}]$ : (a)  $[Ni^{2+} - Asp\alpha, Ala\alpha, Lys\epsilon, His\epsilon]$  environment; (b) schematic geometry of  $[Ni^{2+}N_4]$  complex in the  $x, y, z$  coordinates system of the  $D_{2h}$  point group.

On the other hand, the irreducible representations for  $D_{2h}$  point group of the original  $D_{4h}$  d-orbitals, become:  $a_{1g} \rightarrow d_{z^2}$ ,  $a_{2g} \rightarrow d_{x^2-y^2}$ ,  $b_{1g} \rightarrow d_{xy}$ ,  $b_{2g} \rightarrow d_{xz}$ ,  $b_{3g} \rightarrow d_{yz}$ , [12, Table I].

In  $[Ni^{2+}N_4]$  complex,  $Ni^{2+}$  has a low formal oxidation state, and N ligands are donors. There are two possible types of charge transfer spectra: i) excitation of the lone pair electrons of the donor N to higher unfilled levels, and ii) excitation of filled d-orbital electrons to the empty antibonding  $\pi^*$  orbitals of the "N-ligands chromophores" (Fig.3). The first transitions usually occurs at much higher energies than the observed bands positions, so that it is reasonable to assign the observed absorbance bands as  $d \rightarrow \pi^*$  charge transfer transitions. This electronic transition consists into excitation of filled d-orbital electrons to the empty antibonding ( $\pi^*$ ) orbitals of the "N-ligands chromophore".

To develop the molecular orbital of a complex molecule, e.g. then a central atom is bonded to several identical atoms, the group theory can be used to analyse the symmetry of the orbitals of the non-central atoms, and then combine them with appropriate orbitals of the central atom.

#### 4.2. Molecular orbitals of the N-terminal ligands

The quantitative binding of  $Ni^{2+}$  ion with a N-terminal can be defined by the resonance integral between the d-orbitals of metal and the p-ligand orbitals (which are part of a molecular group) wave functions. It is suitable to assume that in the complex configuration from Fig.4(b), the two  $\alpha N$  atoms are equivalents (as terminals of amide groups), and also  $\epsilon N$  and  $\delta N$  atoms are equivalents (as terminals of amine groups), Fig.3. The valence bonds length of the two categories of N-terminal ligands are different because the lone pair electron contribution to bonding is different. So that, the  $\pi^*$  antibonding orbital energy of the amine group is greater than that of the amide group. Molecular orbitals diagram for original  $N_2$  molecule is shown in Fig.5(a).

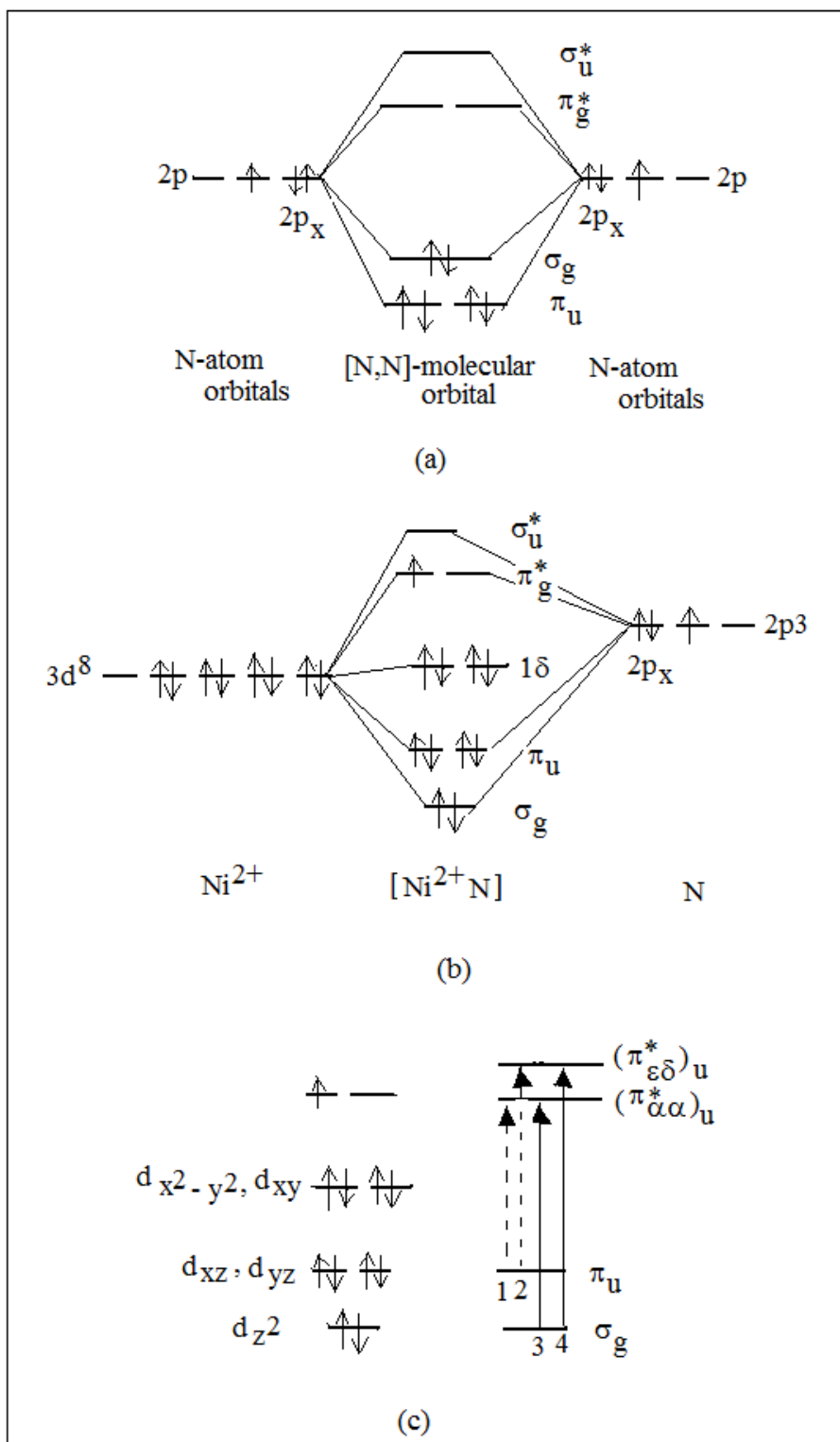


Fig.5. The diagram of the molecular orbitals: (a) ( $p - p$ ) of the ground state  $[N,N]$ -molecular complex; (b) ( $d - p$ ) of the ground state of the  $[Ni^{2+}N_4]$  complex obtained mixing  $3d$ -orbitals of  $Ni^{2+}$  with  $p$ -orbitals of  $N$ ; (c) the assignment of the observed absorbance bands with the charge transfer transitions

The  $p$ -orbital of each  $\alpha\text{N}$  ligand,  $\varphi_{\alpha 1}$  and  $\varphi_{\alpha 2}$ , is part of the antibonding  $\pi^*$ -molecular orbital of the source amide group, while that of  $\varepsilon\text{N}$  or  $\delta\text{N}$  ligand, is part of the antibonding  $\pi^*$ -molecular orbital of the amine group or of the imidazole group, respectively (Fig.3).

Thus, neglecting overlap of the  $\varphi_{\alpha 1}$  and  $\varphi_{\alpha 2}$  antibonding orbitals on  $\alpha\text{N}$ -atoms, we may obtain two empty antibonding  $(\pi^*)_{\alpha\alpha}$  ligand molecular orbitals of the  $[\alpha\text{N}, \alpha\text{N}]$  nitrogen complex, described by two wave functions,  $(\psi_{a\alpha})_g$  out-of-phase combination (lower energy) and  $(\psi_{b\alpha})_u$  in-phase combination (higher energy),

$$\begin{aligned}(\psi_{a\alpha})_g &= \frac{1}{\sqrt{2}}(\varphi_{\alpha 1} - \varphi_{\alpha 2}) \\(\psi_{b\alpha})_u &= \frac{1}{\sqrt{2}}(\varphi_{\alpha 1} + \varphi_{\alpha 2})\end{aligned}$$

Using the same procedure with the same considerations for  $\varepsilon\text{N}$  and  $\delta\text{N}$  ligands, one obtain the wave functions  $(\psi_{a\varepsilon\delta})_g$  out-of-phase combination and  $(\psi_{b\varepsilon\delta})_u$  in-phase combination, of other two empty antibonding  $(\pi^*)_{\varepsilon\delta}$  molecular orbitals of the  $[\varepsilon\text{N}, \delta\text{N}]$  nitrogen complex,

$$\begin{aligned}(\psi_{a\varepsilon\delta})_g &= \frac{1}{\sqrt{2}}(\varphi_{\varepsilon} - \varphi_{\delta}) \\(\psi_{b\varepsilon\delta})_u &= \frac{1}{\sqrt{2}}(\varphi_{\varepsilon} + \varphi_{\delta})\end{aligned}$$

where  $\varphi_{\varepsilon}$  si  $\varphi_{\delta}$  are parts of the  $\pi^*$  antibonding molecular orbital of the amine side-chain lysine group and imidazole group, respectively. Remember that the  $\pi^*$  antibonding orbital of these groups has higher energy than the same orbital of amide group. If we assume that all two  $\alpha\text{N}$ -atoms, and also two  $\varepsilon\text{N}$ ,  $\delta\text{N}$ -atoms, are equivalent in the  $[\text{Ni}^{2+}\text{N}_4]$  complex,  $\varphi_{\alpha 1} \cong \varphi_{\alpha 2}$ ,  $\varphi_{\varepsilon} \cong \varphi_{\delta}$ . Thus, the  $[\text{Ni}^{2+}\text{N}_4]$  complex has two empty antibonding molecular orbitals,  $(\pi^*)_{\varepsilon\delta}$  with higher energy than  $(\pi^*)_{\alpha\alpha}$ , described by the  $(\psi_{b\alpha})_u$  and  $(\psi_{b\varepsilon\delta})_u$  respectively, Fig.5(c).

### 4.3. Molecular orbitals of $[\text{Ni}^{2+}\text{N}_4]$ -complex

The  $[\text{Ni}^{2+}\text{N}_4]$  complex has four bonding molecular orbitals which are mostly ligand character. These orbitals are completely filled as each ligand contributes a (to) pair of electrons. The filling of these orbitals is the source of the stability of the complex.

For the square-coplanar diamagnetic  $d^8$  complex it is of interes only filled d-orbitals, namely  $d_{x^2-y^2}$ ,  $d_{xy}$ ,  $d_{xz}$ ,  $d_{yz}$ . Experimental results for the  $[\text{PtCl}_4]^{2+}$  complexes [26] confirm the theoretical energy order of these orbitals in  $D_{2h}$  symmetry of the complex,  $d_{x^2-y^2} > d_{xy} > d_{xz}, d_{yz}$ . This order is consistent with the formation of molecular orbitals from  $d$ -atomic orbitals of metal and  $p$ -atomic orbitals of ligands:  $d_{z^2}$  forms a  $\sigma$ -bonding orbital,  $d_{xz}$  and  $d_{yz}$  form a  $\pi$ -bonding orbital, and  $d_{x^2-y^2}$  and  $d_{xy}$  form a new  $\delta$ -bonding (with large character of anti-bonding) [27].

Molecular orbitals of the  $[\text{Ni}^{2+}\text{N}_4]$  complex formed from  $3d$ -orbitas of  $\text{Ni}^{2+}$  combined with the  $3p$ -orbitals of N, are:  $1\sigma$  and  $1\pi$  bonding orbitals,  $1\delta$  new non-bonding orbital and  $2\pi^*$  and  $2\sigma^*$  antibonding orbitals, Fig.5(b). The antibonding orbitals will reside predominantly on the atom with greather orbital energy (the less electronegative atom), namely  $\text{Ni}^{2+}$ . Thus, it is plausible that the complexation of the N-terminal atoms induces any length bond changes at their original group.

The positions of the final antibonding orbitals of the  $[\text{Ni}^{2+}\text{N}_4]$  complex,  $(\pi^*)_{\varepsilon\delta}$  and  $(\pi^*)_{\alpha\alpha}$ , result by overlapping between the  $\psi$ -orbitals of the ligands, and  $(d-p)$ -orbitals of metal ion with the same symmetry and their relative energy positions may be evaluated by any resonance integrals of form  $S = \langle d|H|\psi \rangle$ , where  $H$  is the appropriate hamiltonian.

Finally, the observed absorbance bands 1,2,3,4 may be assigned to following transitions: (1)  $d_{xz}, d_{yz} \rightarrow (\psi_{b\alpha})_u$ , (2)  $d_{xz}, d_{yz} \rightarrow (\psi_{b\varepsilon\delta})_u$ , (3)  $d_{z^2} \rightarrow (\psi_{b\alpha})_u$  and (4)  $d_{z^2} \rightarrow (\psi_{b\varepsilon\delta})_u$  (Fig.5(c)); the transitions  $d_{x^2-y^2}, d_{xy} \rightarrow (\psi_{b\alpha})_u$  and  $d_{x^2-y^2}, d_{xy} \rightarrow (\psi_{b\varepsilon\delta})_u$  (not shown in figure) are electric dipole forbidden because the non-bonding  $\delta$ -orbitals ( $d_{x^2-y^2}, d_{xy}$ ) does not overlap to antibonding  $(\psi_{b\alpha})_u$  and  $(\psi_{b\varepsilon\delta})_u$  orbitals. All these transitions are excitations of the  $[\text{Ni}^{2+}\text{N}_4]$  complex formed via a charge transfer from N-terminal ligands to  $\text{Ni}^{2+}$ .

Taking into account symmetry constraints, both the (1) and (2) transitions are dipole moment forbidden (dashed lines), but are placed in the  $\pi \rightarrow \pi^*$ amide groups excitations range that marks the interaction of the frontier molecular orbitals, HOMO and LUMO, of the protein. The blue shift of the intense band (1) of the complex comparing to the free protein, is more probable due to any local conformational changes by complexing of protein, so that the chromophores of protein will differ in their environments. The complex- dipole moment induced by electron-transition from  $d$ -orbital of  $\text{Ni}^{2+}$  to  $\pi^*$ -antibonding N-ligands preferential localised to metal, makes an angle to the chromophore-dipole of protein group and their dipole-dipole interaction increases the transition energy. This behaviour is supported by Woodward and Hoffmann rules [28], which show that by examining the interaction of the frontier molecular orbitals both the local- and stereospecificity could be accounted for.

The (3) and (4) transitions are dipole moment allowed (continuous lines) those intensity depends on formed  $[\text{Ni}^{2+}\text{N}_4]$  complex number. The spectral position of these transitions depends on the nature of side-chain amino acids ligands. Identification, e.g. of a structural rôle of a lysine amino acid is of importance since Ni-albumin is the antigenic determinant recognised by an Ni-specific antibody in nickel allergy.

The transition-dipole—chromophore-dipole interaction induces any major configurational changes of protein, but on the other hand, the metal ions have a preferential coordination tendency with the coordinating side chain of amino acids in protein. We shall analyse the subsequent evolution of the binding metal-protein using time-scanning UV spectra.

## 5. Conclusions

The UV-absorbance of the  $1 \times 10^{-4}\text{M}$  [BSA:  $\text{Ni}^{2+}$ ][1:1] system in phosphate buffer solution is greater than that of free  $1 \times 10^{-4}\text{M}$ [BSA] and the second derivative shows new four bands, at  $\lambda = 236\text{ nm}$ ,  $228\text{ nm}$ ,  $222\text{ nm}$ ,  $210\text{ nm}$ . We propose a model for square-planar  $[\text{Ni}^{2+}\text{N}_4]$  complex of  $\text{Ni}^{2+}$  with four N-terminal, two  $\alpha\text{N}$ ,  $\varepsilon\text{N}$ ,  $\delta\text{N}$ , providing by an Ala, an Asp, an Lys and an His side chain amino acids of BSA. Accommodating the symmetry of this coordination with the symmetry of the  $d$ -orbitals of  $\text{Ni}^{2+}$ , it is reasonable to assign the observed absorbance bands as  $d \rightarrow \pi^*$  charge transfer transitions. This electronic transition consists into excitation of complex filled  $d$ -orbital electrons to the empty antibonding  $(\pi^*)$  orbitals of the N-ligands provided from N-terminals of the protein chromophores.

The identification of a structural role of certain amino acids, as lysine or histidine, for given binding conditions, is of importance for using Ni-albumin system both as diagnose and treatment of specific diseases.

## Acknowledgements

Romanian National Authority for Scientific Research supported this work under the strategic Grant POSDRU 88/ 1.5/ S / 56668.

## References

- [1] Peters, T.Jr. *Adv. Protein. Chem.*, **37**, 161-245 (1985)
- [2] S.L.Wang, S.Y.Lin, M.jane, Y.wei, T.F.Hsieh, *Biophys. Chem.* **111**, 205 (2005).
- [3] M.Luisa Ferrer, Ricardo Duchowicz, Beatriz Carrasco, Jose Garcia de la Torre, and A.Ulises Acuna, *Biophysical Journal* Volume 80, pp 2422-2430, May 2001
- [4] Gregor Blaha, Monira Siam and Harald Lehner, *I.Chem. Soc., Perkin Trans.* **2**, 2119 (1997).
- [5] Jianniao Tian, Jiaqin Liu, Zhide Hu, Xingguo Chen, *American Journal of Immunology* **1**(1), 21-23 (2005).
- [6] Bedabrata Saha, Saswati Chakraborty and Gopal Das, *J.Phys.Chem.C*, **114**(21), 9817-9825 (2010).
- [7] Peter J. Sadler, Alan Tucker and John H. Viles, *Eur. J. Biochem.* **220**,193-200, 1994
- [8] Amit Das, R. Chitra, R.R. Choudhury and M.Ramanadham, *PRAMANA-Journal of Physics, Indian Academy of Sciences*, **63**(2), 363 (2004).
- [9] Carter, D.C., and Ho, J.X., *Adv. Protein. Chem.*, **45**,153 (1994).
- [10] Koichi Murayama and Mihoko Tomida, *Biochemistry*, **43**, 11526-11532 (2004).
- [11] A.P.J. Middelberg, L.He, A.F.Dexter, H.-H. Shen, S.A. Holt and R.K. Thomas, *J.R.Soc.Interface*, **5**, 47-54 (2008).
- [12] B.Bosnich, Contribution from the William Ramsay and Ralph Forster Laboratories, university College, London W.C.1,England, pp 627-632, 1967 si E. Frason, C. Panattoni, and L.Sacconi, *J.Phys. Chem.*, **63**, 1908 (1959).
- [13] Zhou Yongoia, Hu Xuying, Ouyang Di, Huang Jiesheng and Wang yuwen, *Biochem.j.*, **304**, 23-26 (1994).
- [14] Ciro Balestrieri, Giovanni Colonna, Alfonso Giovane, Gaetano Irace, and Luigi Servillo, *Eur. J.Biochim.*, **90**, 433-440 (1978).
- [15] Akihisa Nonoyama, Dissertation, Department of Arts and Sciences, University of South Florida, p 230 pag, 2004
- [16] Leonor Cruzeiro, CCMAR and FCT, University of Algarve, 8000 Faro, Portugal, Oct. 2005, [lhansson@ualg.pt](mailto:lhansson@ualg.pt); [URL:http://w3.ualg.pt/~lhansson](http://w3.ualg.pt/~lhansson)
- [17] N.A. Nevskaya and Yu.N.Chirgadze, *Biopolymers* **15**, 637 (1976).
- [18] R.K.Watt and P.W.Ludden, *CMLS, Cell.Mol.Life Sci.*, **56**, 604-625 (1999).
- [19] Daniel A. Kleier, John H.Hall, Jr., Thomas A Halgren, and William N. Lipscomb, *Proc. Nat. Acad.Sci. USA*, **71**(6), 2265 (1974).
- [20] Wikipedia
- [21] Jayaraman Jayabharathi, Venugopal Thanikachalam, Natesan Srinivasan, Marimuthu Venkatesh Perumal, **84**(1), 233-237 (2011).
- [22] C.R.Cantor & P.R.Schimmel, *Biophysical Chemidtry, PartI: W.H.Freeman and Company*, 1980
- [23] G.P.Smith, Oak Ridge National Laboratory, 1963
- [24] Kunio Takeda, Akira Wada, Kazuo Yamamoto, Yoshiko Moriyama, and Koichiro Aoki, *Journal of Protein Chemistry*, **8**(5), 653-659 (1989).
- [25] H.A.Tajmir-Riahi, *Scientia Iranica*, **14**(2), 87-95 (2007).
- [26] B.Bosnich, *J.Am.Chem.Soc.*, **88**, 2606 (1966).
- [27] Tanya M.Ramond, Gustavo E.Davico, Fredrik Hellberg, Fredrik Svedberg, Peter Salen, Patrick Soderqvist, and W. Carl Lineberger, *Journal of Molecular Spectroscopy*, **216**, 1-14 (2002).
- [28] Wikipedia